Cellulose (2022) 29:5913–5922
https://doi.org/10.1007/s10570-022-04610-w

ORIGINAL RESEARCH

Comparative study on material properties of wood-ash alkali and commercial alkali treated Sterculia fiber

Krishna Prasad Kandel · Menuka Adhikari · Madhav Kharel · Girja Mani Aryal · Shiva Pandeya · Mahesh Kumar Joshi · Bipeen Dahal · Bhoj Gautam · Bhanu Bhakta Neupane

Received: 4 January 2022 / Accepted: 22 April 2022 / Published online: 23 May 2022

Abstract Pulp, paper, and related industries consume large amount of commercial alkali to process raw fiber and/or recycle waste. A low-cost alternative to commercial alkali would be useful to reduce production and recycling costs and global alkali use. In this research, we extracted alkali from wood ash and, as a proof of concept, used the alkali to process lignocellulose fiber obtained from *Sterculia villosa* (locally known as Murgilo or Mudilo), a traditionally important fibrous plant. Material properties of wood-ash alkali (WAA) treated fiber were compared with 5% sodium hydroxide treated fiber. The net weight loss on WAA and sodium hydroxide treatment was found to be 29.1 ± 2.6 and $41 \pm 3.3\%$, respectively. In both methods, the weight loss resulted from the removal of hemicellulose and lignin consistent with reduction of fiber width and weakening of lignin and hemicellulose characteristic bands in FTIR spectra. Interestingly, both methods resulted in fiber having very similar mechanical strength. Cellulose crystallinity, fiber-surface morphology, and thermal stability of cellulose fiber obtained from two methods were systematically compared. These findings suggested that WAA treatment method could be a low-cost method for processing lignocellulose biomass.

Supplementary information The online version contains supplementary material available at https://doi.org/10.1007/s10570-022-04610-w.

K. P. Kandel · M. Kharel · G. M. Aryal · S. Pandeya · M. K. Joshi · B. Dahal · B. B. Neupane (✉)
Central Department of Chemistry, Tribhuvan University, Kathmandu, Nepal
e-mail: bbneupane@cdctu.edu.np; newbhanu@gmail.com

M. Adhikari · B. Gautam
Department of Chemistry, Physics and Materials Science, Fayetteville State University, Fayetteville 28301, NC, USA

Graphical abstract

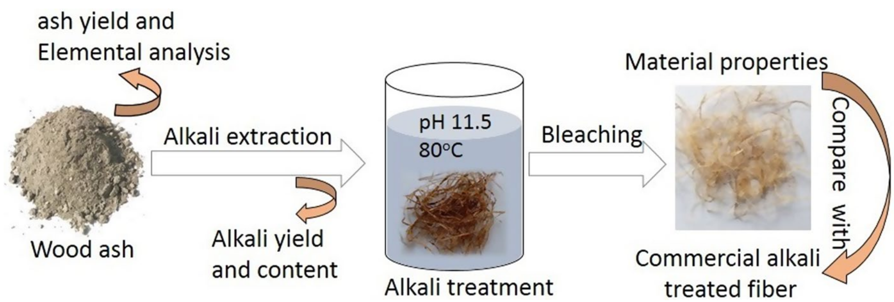

Keywords Lignocellulose · Paper and pulp · Fiber processing · Cellulose fiber · Mechanical strength

Introduction

Lignocellulose fiber is one of the most important materials for paper, pulp, and cardboard industries. The fiber can be obtained from bark, leaf, root and other plant-based materials following chemical and/or mechanical processing (Reddy and Yang 2007; Bajpai 2018; Tanpichai et al. 2019). The processed lignocellulose fibers such as hemp, sisal, coir, kenaf, jute have good thermal stability and specific strength, low density, and are ecofriendly in nature. Such fibers are being explored as a promising alternative to glass- and plastic-based fibers in composite manufacturing. The natural fiber reinforced composite materials offer several advantages and have found important applications in automobile- and agro-based industries, waste water treatment, structural engineering and many more (Vigneshwaran et al. 2020; Dasore et al. 2021).

Major chemical components of unprocessed cellulose fiber are cellulose, hemicellulose, lignin and extractives. Depending on the desired application, raw fiber needs to be processed at different levels following chemical and/or mechanical methods (Bajpai 2018). In chemical treatment method, fiber biomass is cooked in: (a) mixture of sulfurous acid and bisulfite ion (sulfite pulping) or (b) mixture of sodium hydroxide and sodium sulfide (Kraft pulping) or (c) alkali or mixture of alkalis. Pulping, depending on the fiber-treatment conditions, removes non-cellulosic cementing materials (lignin and hemicellulose) and other impurities to different extent so that the effective width of fiber bundle is decreased and the bundles are partially or fully separated. Pulping also changes surface morphology, crystallinity, specific strength and thermal stability of fiber (Saha et al. 2010; Liu et al. 2013; Chandrasekar et al. 2017). Kraft pulping, which is designed to recover energy and cooking chemicals, represents around 75% of all pulp produced and 91% of chemical pulping globally (Bajpai 2015). Small scale or handmade paper industries, normally process fiber using commercial alkali or mixture of alkalis (Banjara 2007; Hubbe and Bowden 2009; Mejouyo et al. 2020; Sannapapamma et al. 2020; Chauhan and Meena 2021).

Waste from paper, pulp, and cardboard industries contributes significantly to water, soil and air pollution (Chakraborty et al. 2019; Gaur et al. 2020; Sharma and Singh 2021). To solve the problem, modern paper and pulp making plants have improved design to recover chemicals, convert residual biomass to higher energy value products or cook the residual biomass for extended period to increase the microbial action (Chakraborty et al. 2019). Any low-cost and environmentally-benign alternative, which can be used in fiber processing and waste recycling, would be very useful to reduce the production cost and global alkali use.

In this study we extracted alkali from wood ash and used it to process raw fiber of *Sterculia villosa*. The net weight loss, fiber width, and surface morphology of wood ash alkali treated fiber were compared with untreated and commercial alkali treated fiber. Mechanical strength, thermal stability, and crystallinity of the cellulose fiber obtained from both methods were also compared systematically. Further implications of the research are also provided.

Materials and methods

Fiber treatment with commercial alkali

The outer scaly bark of raw *Sterculia villosa* fiber was manually removed and air dried. The biomass was refluxed at 80 °C in hexane and methanol mixture (2:1 v/v) for five hours and then boiled in distilled water for four hours. The extractive free and dried fiber was immersed in 5% NaOH solution, keeping fiber mass to alkali volume ratio of 1:50. Temperature of the solution was maintained at 80 ± 2 °C for 4 h. After treatment, the content was cooled to room temperature, neutralized with 5% acetic acid solution, and thoroughly washed with distilled water. The biomass was then treated at room temperature for three hours in 2% H_2O_2 solution (1:30 w/v) prepared in Na_2CO_3 and $NaHCO_3$ buffer of pH 9. The fiber was washed several times with distilled water and dried at 100 ± 5 °C till constant weight was obtained. From the initial and final weights of fiber, weight loss in percentage was calculated. The sample prepared by this method is hereunder named as NaOH-treated sample.

Wood ash alkali extraction and fiber treatment

Wood ash was obtained by burning dry Dalbergia sissoo (locally named as Sissau) tree wood and branches in a homemade oven at around 600 °C. Ash yield was found to be around 7%. The ash was sieved through 500 µm sieves. 40 g of sieved and dry ash was added to a liter of distilled water, the solution was stirred for 2 h, and then allowed to decant for 30 min. The supernatant was filtered through Whatman 40 filter to get ash solution (hereafter named as wood ash alkali; WAA). The pH of WAA solution was found to be 11.5 ± 0.1. The concentration of alkali, as determined by titration and pH measurement methods, was found to be 3×10^{-3} M (0.02% w/v). In calculation, it was assumed that alkalinity is due to $Ca(OH)_2$; the evidence is provided in results and discussion section. Alkali yield was found to be 0.2% on dry ash basis (w/w).

The extracted wood ash alkali was further used for treatment of extractive free *Sterculia villosa* fiber. Treatment procedure was the same as reported in Sect. 2.1 for NaOH treatment method. As before, from the known initial and final weights, percentage weight loss was calculated. Sample prepared by this method is hereafter referred to as WAA-treated sample. A simple schematic diagram of the fiber processing method is provided in Fig. 1.

Estimation of cellulose, hemicellulose, and lignin

Cellulose, lignin and hemicellulose in extractive-free and untreated Sterculia fiber sample was estimated gravimetrically following the methods reported in literature (Boopathi et al. 2012; Das et al. 2014; Adeeyo et al. 2015). For cellulose estimation, 1.00 g of dry fiber was treated with 5% NaOH (w/v) with the ratio of 1:30 at 80 °C for 5 h. The content was allowed to cool and neutralized with 10% sulfuric acid. The residual biomass was vacuum-filtered using Whatman 40 filter paper using Buchner funnel. The biomass was then treated for 5 h at room temperature with 2% H_2O_2 solution (fiber biomass to H_2O_2 mass volume ratio 1:30) prepared in Na_2CO_3 and $NaHCO_3$ buffer of pH 9. The content was stirred using a magnetic stirrer for 5 h until the fiber was bleached completely. The biomass was washed and dried multiple times until a constant weight was obtained. The initial and

Fig. 1 A simple schematic of WAA treatment method. Major steps followed in the treatment method are also indicated

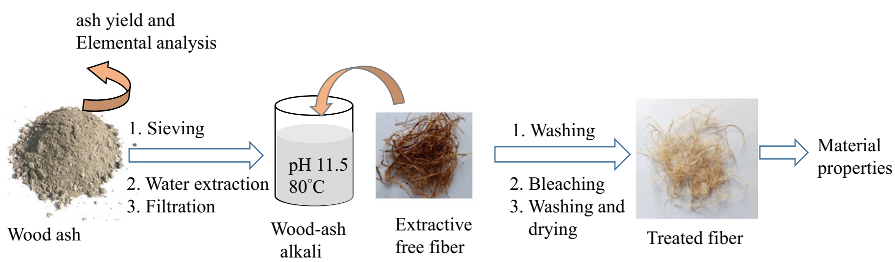

final biomass weights were used to get cellulose content in percentage.

To determine hemicellulose, 1.000 g of dry extractive-free untreated fiber was added in 2.5% NaOH solution by maintaining fiber mass to alkali volume ratio of 1:50. The content was boiled for 4 h. The content was cooled, neutralized after several washing with distilled water, filtered and dried at 105 °C till constant weight was obtained. From the initial and final dry weights, hemicellulose content in % was measured.

For lignin estimation, 1.000 g of extractive-free untreated fiber was added in 72% H_2SO_4 by maintaining fiber weight to acid volume ratio of 1:12.5. The content was carefully stirred for 2 h and the supernatant was removed after several dilution and washing. The residue was filtered and dried at 105 °C till constant weight was obtained. From the initial fiber and final dry fiber weights lignin content was calculated.

For comparison, estimation of cellulose, hemicellulose and lignin was also made in WAA-and NaOH-treated samples.

Measurement of fiber width

The fiber sample was imaged using a digital bright field microscope (AmScope, 5-250X, USA). The field of view was calibrated by a high precision linear calibration grid having smallest grid size of 10 µm. From the known size of pixel in micrometer, fiber width was measured in an open-source image analysis software (ImageJ, NIH, USA).

FTIR, XRD, DTA, and SEM measurements

The IR spectra were collected in attenuated total reflection (ATR) mode at resolution 4 cm^{-1} in 4000–400 cm^{-1} range using a Fourier transform infrared spectrometer (ABB Bomen, MB100, Canada). Before measurement, each fiber sample was pre-conditioned for 12 h at 23 ± 1 °C and 60% RH. To get good signal to noise ratio, each spectrum was reported as the average of 30 optical scans.

XRD data were measured at 30 kV, scan rate 0.02°/min, step size 0.02° in the 2θ range of 5−50° using Rigaku MiniFlex600 X-ray diffractometer. Monochromatic X-ray source obtained from Cu Kα line (λ = 1.540 A°) was used in the measurement.

For thermogravimetric analysis (TGA) 7−10 mg of sample was heated in alumina crucible (Perkin Elmer, TGA-7) in the temperature range of from 26 to 600 °C at constant heating rate of 10 °C/minute under nitrogen atmosphere (flow rate of 80 mL/min). Temperature precision and balance accuracy were ± 2 °C and 0.1 µg, respectively.

Scanning electron microscopic images of the samples were collected at 15 kV accelerating voltage using a JEOL JXA-8530 F field-emission electron probe microanalyzer (EPMA), equipped with an X-ray energy-dispersive spectrometer (EDS) for chemical compositional analysis. For each sample, 4−6 SEM images were collected at magnification of 50−5000X. Image analysis was done in ImageJ (ImageJ, NIH, USA) to get information on fiber surface morphology.

Mechanical strength of fiber

The untreated and alkali-treated fiber samples were preconditioned at 23 ± 1 °C and 65% RH for 24 h following ASTM test method (ASTM 2004). Fiber strength was measured using a fiber bundle strength tester (TSI instruments) having maximum load capacity of 7 kg. For measurement, flat fiber bundles were loaded in Pressley Jaw (gauze length 15 mm) and then the assembly was loaded in the tester. Load was applied at constant loading rate of 1 kg/sec till the fiber breaks. The load at fiber break was noted along with percentage elongation. The broken fiber was removed from Pressley Jaw and weighed in an analytical balance (nearest accuracy of 0.0001). From the known value of breaking load, grammage, and length of fiber bundle (which is 1.5 cm), fiber bundle strength (breaking tenacity) in g/tex and tensile strength were calculated. Seventy-five measurements were made for each sample type to make the result statistically significant.

Table 1 Chemical characterization of fiber samples

Sample type	Weight loss	Cellulose	Hemicellulose	Lignin
Untreated	0	55.6 ± 2.4	28.2 ± 1.7	19.7 ± 2.5
WAA treated	29.1 ± 2.6	72.0 ± 1.9	18.2 ± 1.2	9.9 ± 1.4
NaOH treated	41.3 ± 3.3%	82.1 ± 1.3	12.5 ± 1.7	8.4 ± 1.1

Statistical analysis

The data collected were analyzed in Microsoft Excel spreadsheet to get basic statistical parameters such as mean, standard deviation, and confidence interval. Whenever required, paired t-test between the different data sets was performed in OriginPro (OriginLab Corporation, USA).

Results and discussion

Weight loss, chemical characterization, and fiber width

The % (w/w) of cellulose, hemicellulose and lignin in dry and extractive-free untreated fiber was found to be 55.6 ± 2.4, 28.2 ± 1.7, 19.7 ± 2.5, respectively. Since the analysis was made in extractive-free and dry biomass, the weight% of three components adds to 100%. One of the commonly used chemical processing methods for lignocellulose fiber in laboratory and industrial settings involves 5% NaOH treatment (w/v) at elevated temperature followed by chlorine free bleaching. So, it would be more reasonable to compare material properties of fiber processed by this method (NaOH treatment method) with WAA treated fiber. The net weight loss measured from the biomass after NaOH and WAA treatment was found to be 41.3 ± 3.3% and 29.1 ± 2.6; respectively (Table 1). In both methods, the major contribution to weight loss is due to removal of hemicellulose and lignin on alkali treatment. Alkaline H_2O_2 bleaching is used as relatively safe bleaching method to remove residual lignin and colorants from the fiber. This could contribute to minor weight loss. As expected, bleaching resulted in significant increase in fiber brightness (Fig. 1).

The treatment parameters, except the alkali concentration, were same in both methods. The lower weight loss on WAA treatment is due to lower concentration of alkali. Literature studies have reported that the weight loss depends on nature of alkali solution and treatment parameters such as, concentration, time, and temperature (Saha et al. 2010; Hashim et al. 2017). In both methods, consistent with weight loss study, cellulose content increased whereas the hemicellulose and lignin content decreased (Table 1).

To further explore the effect of alkali treatment, fiber width was also measured in all the samples.

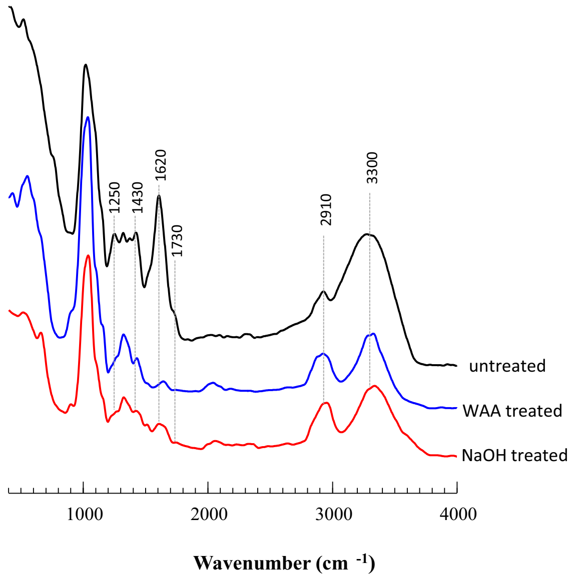

Fig. 2 FTIR spectra of untreated and NaOH and WAA treated fibers. For easy comparison, the spectra as flipped to show absorption bands and overlaid vertically

The mean fiber bundle width (n = 275) at 95% CI for untreated, WAA treated and NaOH treated samples was measured as 446.0 ± 40.2, 227.0 ± 25.0, and 227.9 ± 20.0 µm, respectively. Consistent with the data reported in Table 1, the decrease in fiber width in alkali treated samples is due to removal of lignin, hemicellulose, and other materials from the fiber. Reduction in fiber width on alkali treatment is also reported for other plant fibers (Beckermann and Pickering 2008; Han et al. 2009; Hashim et al. 2017).

To get information on elemental composition of wood ash, SEM, SEM-EDX, and XRD data were measured. EDX data showed (Fig. S2 and Table S1) significant amount of calcium (22.3%) along with C (23%), O (50.5%), Al (1%), and Fe (1.4%), and Si (1.8%). Sources of calcium could be $CaCO_3$ and $Ca(OH)_2$ or their decomposition product CaO. Al, Fe, and Si could originate from silicate minerals. The XRD data (Fig. S3) also showed characteristics peaks of $CaCO_3$ (2θ = 29.4°, 39.5°, 43.2°, 48.5°) (Kontoyannis and Vagenas 2000) $Ca(OH)_2$ (2θ = 28.6°, 47.5°, 48.5°), and CaO (2θ = 32°, 64.7°) (Khachani et al. 2014). The alkaline property of ash solution is due to CaO and $Ca(OH)_2$ present in the wood ash.

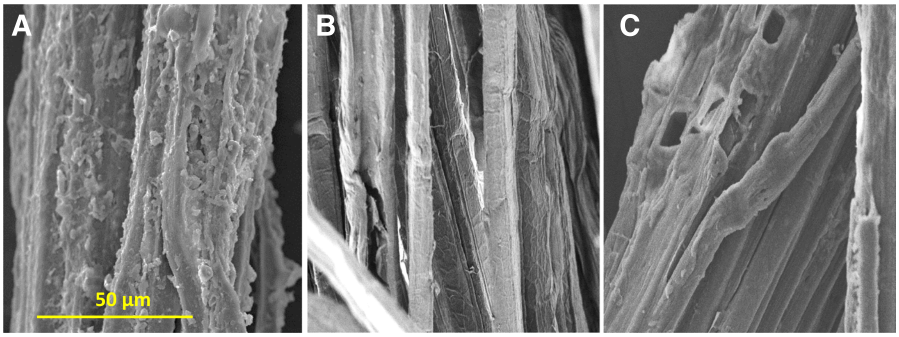

Fig. 3 SEM images of **A** untreated, B WAA treated, and **C** NaOH treated fibers. A scale bar of 50 µm shown in figure A also applies for B and C

FTIR study

FTIR data of all the samples is provided in Fig. 2. Spectral assignments of each band was made on the basis of literature provided information. The broad peak in the range of 3000–3600 cm^{-1} is attributed to O−H stretching of hydrogen bonded networks in cellulose and hemicellulose (Sinha and Rout 2008; Saha et al. 2010). The reduction in intensity and width of the band in alkali treated samples is due to breaking of hydrogen bond between O–H groups of hemicellulose and cellulose molecules resulted from partial removal of hemicellulose. A peak at 1730 cm^{-1} is linked to acetyl or ester C=O groups of (non-conjugated) hemicellulose or lignin and at 1620 to C=O stretching of conjugated lignin (Haque et al. 2009; Tanpichai et al. 2019). These peaks become weak on alkali treatment indicating removal of hemicellulose and lignin. A characteristic peak at 1250 cm^{-1}, which corresponds to C–O stretching of acetyl groups of cellulose and hemicellulose, is also weekend on alkali treatment (Sinha and Rout 2008). This also indicates the hemicellulose removal. These observations are consistent with the weight loss data reported in Table 1. A peak at 1430 cm^{-1}, which corresponds to CH_2 bending of cellulose, becomes slightly weaker in NaOH treated sample and remains intact in WAA treated sample. These unaffected cellulose could help to preserve mechanical strength in the alkali treated fiber (Sui et al. 2009; Saha et al. 2010).

SEM imaging

The fiber surface of untreated sample showed additional materials deposited on the fiber surface (Fig. 3A). These materials could be residual wax, pectin, inorganic impurities along with cementing

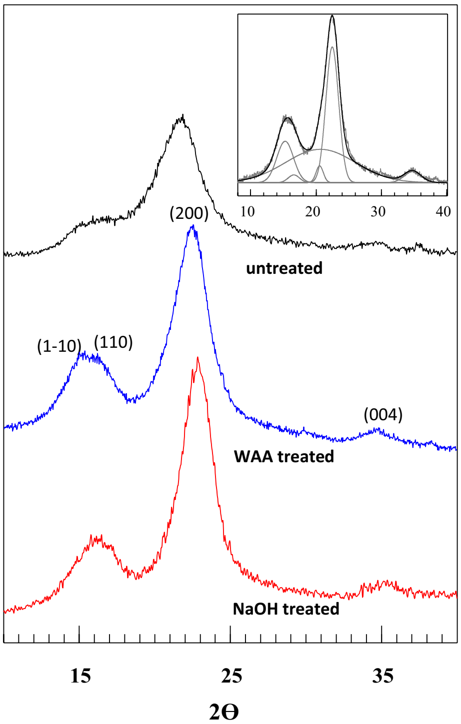

Fig. 4 XRD data of untreated, WAA treated, and NaOH treated fibers. For easy composition data are overlaid vertically. The inset shows a six components fit to the XRD data of WAA treated fiber

Table 2 Crystalline properties of the fiber samples

Sample type	Crystallinity index (%)	Crystallite size (nm)	d_{200}, nm	Micro-strain
Untreated	47	3	0.406	0
WAA treated	55	3.7	0.394	−0.031
NaOH treated	57.9	3.7	0.388	−0.015

materials such as lignin and hemicellulose. On alkali treatment, majority of the materials are removed from the surface (Fig. 3B and C). Also, fiber bundles are partially separated due to the removal of cementing materials. These observations are consistent with the weight loss, reduction of fiber width, and weakening of lignin and hemicellulose characteristic peaks in FTIR data reported in earlier sections. Partial fibrillation is also observed in the alkali-treated samples (Fig. 3B and C) due to removal of cementing materials from inter-fibrillar region. Micro cracks, which are formed along the length of the fiber, are also visible in the alkali treated sample images.

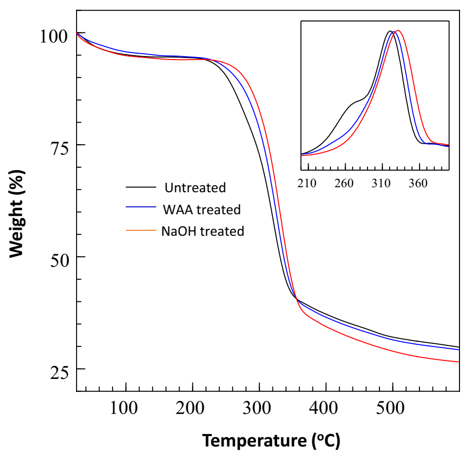

Fig. 5 Thermogravimetric analysis. The main frame and inset show the TGA and DTG data of three fiber samples; respectively

XRD analysis

Figure 4 shows the XRD data of all the samples. The diffraction peaks at 2θ angles of 15.5°, 21.5°, and 35° originate from (1–10) and (110), (200), and (004) planes of crystalline cellulose phase I; respectively. A broad contribution underlying the crystalline peaks originates from amorphous scattering (Park et al. 2010). A six-component peak deconvolution (inset in Fig. 4) in the 2θ range of 5–40° was used to get information on crystallinity index (*CI*) (Park et al. 2010; Yao et al. 2020). *CI* was calculated using Eq. 1.

$$CI = \left(\frac{A_t - A_{am}}{A_t}\right) \times 100 \tag{1}$$

where A_t and A_{am} are the integrated intensity of both crystalline and non-crystalline phases and non-crystalline phases only; respectively. Gaussian and Voigt profiles were used for crystalline and non-crystalline or amorphous contributions (French 2020; Yao et al. 2020). Before deconvolution, a two-point baseline correction was done to subtract the instrumental background. This correction ensures that the intensity far from crystalline peak position is zero (2θ at 5° and 40°) (Yao et al. 2020). The CI in untreated, WAA, and NaOH treated samples was found to be ~ 47%, ~ 55% and ~ 58%; respectively (Table 2). The CI

Table 3 A summary of weight loss data for the fiber samples

Sample type	ΔT, °C	Mass loss, %	Degradation temperature, °C	Residual mass at 600 °C, %
Untreated	26–100	4.9	321	29.8
	100–220	4		
	220–400	57		
	400–600	7.4		
WAA treated	26–100	4.2	326	29.4
	100–220	1.5		
	220–400	57.8		
	400–600	7.1		
NaOH treated	26–100	5.1	332	26.5
	100–220	1.2		
	220–400	59.8		
	400–600	7.9		

increase is due to removal of amorphous components such as lignin and hemicellulose, particularly from inter-fibrillar region, followed by reorganization of cellulose chains, as reported in several studies (Park et al. 2010; Saha et al. 2010; Boopathi et al. 2012).

XRD data were further analyzed to calculate micro-strain (ε) in the crystallites in direction perpendicular to the diffracting plane using the following equation (Sinha and Rout 2008; Ioelovich 2018):

$$\varepsilon = \frac{d_s - d_u}{d_u} \tag{2}$$

where d_s and d_u are the inter-planar spacing in strained (alkali treated) and unstrained (untreated) samples. The negative value of ε in the treated sample (Table 2) suggests that residual compressive stress is present on the crystallite surface.

Crystallite size (D) calculated using Scherrer equation (Cullity 1978) is also provided in Table 2. It is found that crystallite size increases by approximately 23% in alkali-treated samples.

Thermal properties

The TGA and DTG data are provided in Fig. 5 and the inset, respectively. To account for the small offset in weight % from 100 (in the range of 2–2.5%), TGA data were normalized to 100. The shape of TGA curve for all samples is similar to a typical lignocellulose fiber sample reported in literature (Poletto et al. 2014). For easy comparison, the % weight loss in different temperature window is summarized in Table 3. The initial weight loss below 100 °C is due to loss of water molecules and or volatile impurities adsorbed on the fiber. A small difference in weight loss at T ≤ 100 °C could be linked to crystallinity change and difference in equilibrium moisture content. A shoulder around ~300 °C in DTG (Fig. 5 inset) is mainly due to degradation of hemicellulose (Poletto et al. 2014). The shoulder is more pronounced in untreated sample suggesting that the sample contains higher amount of hemicellulose. This observation is consistent with FTIR and chemical analysis data reported in earlier sections. Lower thermal stability of hemicellulose is attributed to its amorphous nature leading to de-polymerization at lower temperature (Yang et al. 2006).

It is suggested that cleavage of glycosidic linkage takes place in the range of 275–350 °C. So, the main peak in DTG is attributed to cellulose degradation (Yang et al. 2006). The higher thermal stability of cellulose as compared to hemicellulose is due to well organized and long polymeric units. The cellulose degradation temperature for untreated, WAA treated, and NaOH treated sample was found to be 321 °C, 326 °C, and 332 °C; respectively (Table 3). This suggested that thermal stability is increased on alkali treatment. The higher thermal stability of the treated sample could be due to increased crystallinity and grain size. Lignin degradation is suggested to take place in broad temperature range from 200 to 600 °C and cleavage. The higher thermal stability of lignin is attributed to highly cross-linked structure of high molecular mass. The higher residual mass in untreated sample may be due to inorganic impurities and or formation of stable lignin-cellulose complex (Kim et al. 2006).

Table 4 Mechanical properties of fiber samples

Sample type	Breaking tenacity (g/tex)	Tensile strength, MPa	Elongation at break, %
Untreated	22.8 ± 7.6	319.2 ± 105.8	4.4 ± 1.8
WAA treated	23.1 ± 5.6	323.5 ± 78.5	2 ± 0.8
NaOH treated	21.6 ± 7	302.8 ± 97.2	1.24 ± 0.4

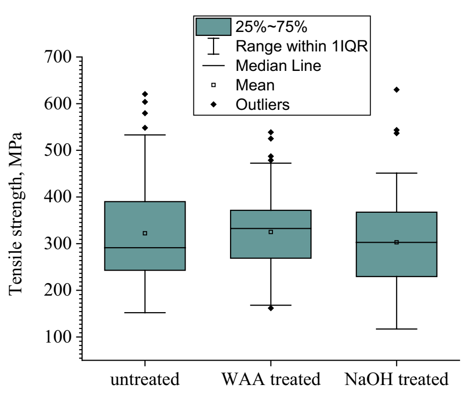

Fig. 6 Tensile strength of the fiber samples. For easy comparison, range, mean, and median values along with few outliers are shown in a box plot

Mechanical strength

The mechanical properties of the fiber samples are provided in Table 4. For easy comparison, tensile strength data (MPa) are plotted in Fig. 6. The mean difference in breaking tenacity and tensile strength of untreated and WAA treated samples are statistically insignificant ($p > 0.01$). Also, tenacity and tensile strength values of untreated and NaOH treated samples are insignificant ($p > 0.01$). The mean difference in percentage elongation is statistically significant in all samples ($p < 0.01$); that is percentage elongation is decreased on alkali treatment.

It is reported that the mechanical strength of alkali-treated samples, depending on treatment conditions, is retained or increased or decreased (Saha et al. 2010; Liu et al. 2013; Chandrasekar et al. 2017; Hashim et al. 2017). It is suggested that the removal of hemicellulose and lignin from inter-fibrillar region decreases the internal constraint and therefore facilitates better organization of microfibrils and cellulose chains. This can result in increase in crystallinity and improvement of strength. The SEM images show that lignin is removed from inter-fibrillar region along with few local damage on the fiber surface (Fig. 3B and C). Alkali- and/or bleach-caused fiber damage can decrease the strength. These two opposing effects could help to retain strength in the treated samples, rather than a significant increase in strength.

Further implications of the research

In this study, material properties of Sterculia fiber treated with wood ash alkali and commercial alkali were systematically compared. Further research could include the fabrication of paper sheets and composite materials using the fiber samples and comparison of their end properties. The concentration of alkali in this work was low, however, the solution could be concentrated following evaporation at reduced pressure. The alkali solution, both in diluted and concentrated forms, could also be useful to neutralize acidic waste and valorize the waste materials in paper and pulp industries. Although we used specific wood ash to process Sterculia fiber, we believe that alkali extracted from any wood ash waste can be used to process lignocellulose fiber. Health risk associated with the handling of wood ash is lower than the commercial alkali. In these respects, the method reported here can be an eco-friendly alternative for processing lignocellulose fiber.

Conclusions

To summarize, we extracted alkali solution from wood ash and used it to process lignocellulose fiber obtained from *Sterculia villosa*. Several important material properties such as weight loss, fiber width, fiber morphology, mechanical strength, thermal stability, and crystallinity of the wood ash alkali treated fiber were compared with untreated and commercial alkali-treated fibers. We found significant removal of lignin and hemicellulose both in WAA and NaOH treatment methods. The tensile strength and breaking tenacity of the fiber obtained from both methods were very comparable. Thermal stability and crystallinity of the fibers obtained from both methods was increased as compared to untreated samples. These findings suggested that wood ash alkali can be used to process lignocellulose fiber on a laboratory scale. Also, the method could be utilized in chemical processing of lignocellulose biomass in small-scale paper and pulp industries.

Funding This work was supported by university, Grants, commission, Nepal (to BBN and KPK; grants # FRG-76/77-S&T-3 and PhD-76/77-S&T-10), and by NSF EIR ECCS 1900837 (BG). The authors would like to acknowledge Dr. Zhiping Luo from Fayetteville State University for providing IMREL facility. The EPMA instrumentation was acquired through U.S. Department of Defense (grant # W911NF-09-1-0011).

Declarations

Conflict of interest The authors declare that there is no conflict of interest.

References

Adeeyo OA, Oresegun OM, Oladimeji TE (2015) Compositional analysis of lignocellulosic materials: Evaluation of an economically viable method suitable for woody and non-woody biomass. Am J Eng Res 4:14–19

ASTM (2004) ASTM D1776–04, Standard practice for conditioning and testing textiles. American Society for Testing and Materials, West Conshohocken, Pennsylvania

Bajpai P (2015) Basic overview of pulp and paper manufacturing process. In: Bajpai P (ed) Green chemistry and sustainability in pulp and paper industry. Springer, Cham, pp 11–39

Bajpai P (2018) Brief description of the pulp and papermaking process. In: Bajpai P (ed) Biotechnology for pulp and paper processing. Springer, Singapore, pp 9–26

Banjara G (2007) Handmade Paper in Nepal: Upgrading with Value Chain Approach. GTZ/PSP-RUFIN

Beckermann GW, Pickering KL (2008) Engineering and evaluation of hemp fibre reinforced polypropylene composites: fibre treatment and matrix modification. Compos A: Appl Sci Manuf 39:979–988

Boopathi L, Sampath PS, Mylsamy K (2012) Investigation of physical, chemical and mechanical properties of raw and alkali treated Borassus fruit fiber. Compos B: Eng 43:3044–3052

Chakraborty D, Dahiya S, Amulya K et al (2019) Valorization of paper and pulp waste: opportunities and prospects of biorefinery. In: Prasad MNV, Favas PJ de C, Vithanage M, Mohan SV (eds) Industrial and municipal sludge. Elsevier, pp 623–656

Chandrasekar M, Ishak MR, Sapuan SM et al (2017) A review on the characterisation of natural fibres and their composites after alkali treatment and water absorption. Plast Rubber Compos 46:119–136

Chauhan S, Meena BL (2021) Introduction to pulp and paper industry: global scenario. Phys Sci Rev 6:81-109

Cullity B (1978) Elements of X-ray diffraction. Addision wisely Publishing Company Inc., London

Das AM, Ali AA, Hazarika MP (2014) Synthesis and characterization of cellulose acetate from rice husk: eco-friendly condition. Carbohydr Polym 112:342–349

Dasore A, Rajak U, Balijepalli R et al (2021) An overview of refinements, processing methods and properties of natural fiber composites. Proc Mater Today

French AD (2020) Increment in evolution of cellulose crystallinity analysis. Cellulose 27:5445–5448

Gaur VK, Sharma P, Sirohi R et al (2020) Assessing the impact of industrial waste on environment and mitigation strategies: a comprehensive review. J Hazard Mater 398:123019

Han G, Cheng W, Deng J et al (2009) Effect of pressurized steam treatment on selected properties of wheat straws. Ind Crops Prod 30:48–53

Haque MM, Hasan M, Islam MS, Ali ME (2009) Physico-mechanical properties of chemically treated palm and coir fiber reinforced polypropylene composites. Bioresour Technol 100:4903–4906

Hashim MY, Amin AM, Marwah OMF et al (2017) The effect of alkali treatment under various conditions on physical properties of kenaf fiber. In: Journal of Physics: Conference Series. IOP Publishing, p 012030

Hubbe MA, Bowden C (2009) Handmade paper: a review of its history, craft, and science. BioResources 4:1736–1792

Ioelovich M (2018) Determination of distortions and sizes of cellulose nanocrystallites. Res J Nanosci Eng 2:1–5

Khachani M, El Hamidi A, Halim M, Arsalane S (2014) Non-isothermal kinetic and thermodynamic studies of the dehydroxylation process of synthetic calcium hydroxide Ca (OH) 2. J Mater Environ Sci 5:615–624

Kim H-S, Kim S, Kim H-J, Yang H-S (2006) Thermal properties of bio-flour-filled polyolefin composites with different compatibilizing agent type and content. Thermochim Acta 451:181–188

Kontoyannis CG, Vagenas NV (2000) Calcium carbonate phase analysis using XRD and FT-Raman spectroscopy. Analyst 125:251–255

Liu H, You L, Jin H, Yu W (2013) Influence of alkali treatment on the structure and properties of hemp fibers. Fibers Polym 14:389–395

Mejouyo PW, Nkemaja ED, Beching OR et al (2020) Physical and Tensile Properties of Handmade Sida rhombifolia Paper. Int J Biomater 2020

Park S, Baker JO, Himmel ME et al (2010) Cellulose crystallinity index: measurement techniques and their impact on interpreting cellulase performance. Biotechnol Biofuels 3:1–10

Poletto M, Ornaghi HL, Zattera AJ (2014) Native cellulose: structure, characterization and thermal properties. Materials 7:6105–6119

Reddy N, Yang Y (2007) Natural cellulose fibers from switchgrass with tensile properties similar to cotton and linen. Biotechnol Bioeng 97:1021–1027

Saha P, Manna S, Chowdhury SR et al (2010) Enhancement of tensile strength of lignocellulosic jute fibers by alkali-steam treatment. Bioresour Technol 101:3182–3187

Sannapapamma KJ, Mariyappanavar S, Sangannavar VV et al (2020) Development and quality assessment of handmade papers using underutilized agro based natural fibres. J Pharmacogn Phytochem 9:1410–1417

Sharma P, Singh SP (2021) Pollutants characterization and toxicity assessment of pulp and paper industry sludge for safe environmental disposal. In: Haq I, Kalamdhad AS (eds) Treatment technologies for waste management. Springer, pp 207–223

Sinha E, Rout SK (2008) Influence of fibre-surface treatment on structural, thermal and mechanical properties of jute. J Mater Sci 43:2590–2601

Sui G, Fuqua MA, Ulven CA, Zhong WH (2009) A plant fiber reinforced polymer composite prepared by a twin-screw extruder. Bioresour Technol 100:1246–1251

Tanpichai S, Witayakran S, Srimarut Y et al (2019) Porosity, density and mechanical properties of the paper of steam exploded bamboo microfibers controlled by nanofibrillated cellulose. J Mater Res Technol 8:3612–3622

Vigneshwaran S, Sundarakannan R, John KM et al (2020) Recent advancement in the natural fiber polymer composites: a comprehensive review. J Clean Prod 277:124109

Yang H, Yan R, Chen H et al (2006) In-depth investigation of biomass pyrolysis based on three major components: hemicellulose, cellulose and lignin. Energy Fuels 20:388–393

Yao W, Weng Y, Catchmark JM (2020) Improved cellulose X-ray diffraction analysis using Fourier series modeling. Cellulose 27:5563–5579